Microporous Materials

DOI: 10.1002/anie.201206557

Enhancement of Activity and Selectivity in Acid-Catalyzed Reactions by Dealuminated Hierarchical Zeolites**

Petr Sazama, Zdenek Sobalik, Jiri Dedecek, Ivo Jakubec, Vasile Parvulescu, Zdenek Bastl, Jiri Rathousky, and Hana Jirglova*

High-silica zeolites with crystalline aluminosilicate frameworks balance the charge of strongly acidic protons during the processing of oil, in petrochemistry, and increasingly in numerous organic syntheses. The transformation of hydrocarbons is controlled by the concentration and strength of the acid sites and the dimensions and architecture of the inner pores. Zeolite micropores, which have a diameter similar to organic molecules, govern the shape selectivity of the reaction in the inner space, but also result in slow transport of reactants and products, thus limiting the reaction rate.[1] Several approaches have been developed to enhance the mass transport by using zeolite nanosheets and nanocrystals,[2–4] or zeolites that contain both micro- and mesopores. The latter hierarchical zeolites were prepared by confined crystal growth,[5,6] by using polymers as mesoporogens,[7] or through post-synthesis desilication or dealumination processes.[8–11] The advantage of the presence of mesopores is, however, accompanied by the nonshape-selective environment of the acid sites located in the mesopores. Our interest in the effective formation of secondary mesoporosity through post-synthesis alkaline treatment of conventional zeolites[12] prompted us to study the potential of leaching procedures for the preparation of hierarchical zeolites, preserving the shape-selective environment of the active sites. The main principles of forming mesopores in high-silica zeolites through alkaline leaching have been described by Groen et al.[10] They demonstrated that dissolution of Si depends mainly on the Al concentration in the framework and occurs in the Si-rich areas. Al atoms partly remain at the framework sites and partly form extra-framework Al species in the mesopores. Groen et al.[10,13] and Caicedo-Realpe and Perez-Ramirez[14] have shown that the formed Al species can be removed by treatment with mild acid, thus restoring the original Si/Al ratio. This treatment increased the isomerization of *o*-xylene, however, the selectivity for *p*-xylene did not reach that of parent microporous zeolites.[13] This study is primarily concerned with the elimination of both the extra-framework and framework Al species, and thus the related acid sites from the mesopores of the desilicated zeolites by employing oxalic acid. The advantage of hierarchical zeolites with acid sites predominantly located in the confined reaction space of the micropores is demonstrated on acid-catalyzed reactions controlled by shape-selectivity effects.

TEM images of the alkaline- and subsequently acid-leached zeolites are given in Figure 1. They clearly show that the treatment resulted in the extensive formation of a secondary mesoporous structure, which is characterized by numerous crystal cavities, which are more populated in ZSM-5 (Si/Al = 22.2) compared to mordenite (MOR, Si/Al = 12.1). The adsorption isotherms of treated ZSM-5 zeolites (Figure 2) indicate adsorption in the zeolite micropores and an H3 hysteresis loop typical for slit-shaped mesopores. But the extensive formation of a mesoporous structure also resulted in a decrease in the micropore volume. Treatment with oxalic acid further extended the mesopore volume and the micropore volume increased, with the final value only slightly lower compared to the parent zeolite. Al plugs, which were formed in the mesopores after desilication and blocked parts of the micropores, were removed by acid leaching, similar to results of Caicedo-Realpe and Perez-Ramirez.[14] With mordenite, alkaline and acid leaching resulted in similar textural changes and led to well-developed secondary mesoporosity with preserved high micropore volumes. The dealuminated zeolite surface was analyzed by XPS monitoring of the relative concentration of Al to Si in the zeolite (sub)surface layers ($\approx$50 Å) by the Al 2p and Si 2p electron levels. The surface Si/Al ratio of both desilicated ZSM-5 and mordenite zeolites compared to the bulk composition (Table 1) indicated accumulation of Al species on the external crystal surface. In contrast, zeolites treated with oxalic acid resulted in a slight surface enrichment in Si. Analysis of the Brønsted and Lewis acid sites of dealuminated micro-mesoporous zeolites indicated predominant Brønsted acidity corresponding to the concentration of Al in the framework (Table 1). The population of acid sites in the dealuminated micro-mesoporous (deAlmm) ZSM-5(I) was analyzed using the FTIR spectra of adsorbed 2,6-ditertbutylpyridine (DTBPy), the kinetic diameter of which (10.5 Å) does not allow it to penetrate into the

[*] Dr. P. Sazama, Prof. Dr. Z. Sobalik, Dr. J. Dedecek, Dr. Z. Bastl, Dr. J. Rathousky, Dr. H. Jirglova
J. Heyrovský Institute of Physical Chemistry
Academy of Sciences of the Czech Republic
18223 Prague 8 (Czech Republic)
E-mail: petr.sazama@jh-inst.cas.cz
Dr. I. Jakubec
Institute of Inorganic Chemistry
Academy of Sciences of the Czech Republic
Husinec-Rez, 25068 Rez (Czech Republic)
Prof. Dr. V. Parvulescu
University of Bucharest
Department of Organic Chemistry and Catalysis
B-dul Regina Elisabeta 4–12, 030016 Bucharest (Romania)

[**] This study was supported by the Czech Science Foundation (project number P106/11/0624), the Ministry of Industry and Trade of the Czech Republic (project number FR-TI3/316), and by RVO number 61388955.

Supporting information for this article is available on the WWW under http://dx.doi.org/10.1002/anie.201206557.

© 2013 Wiley-VCH Verlag GmbH & Co. KGaA, Weinheim

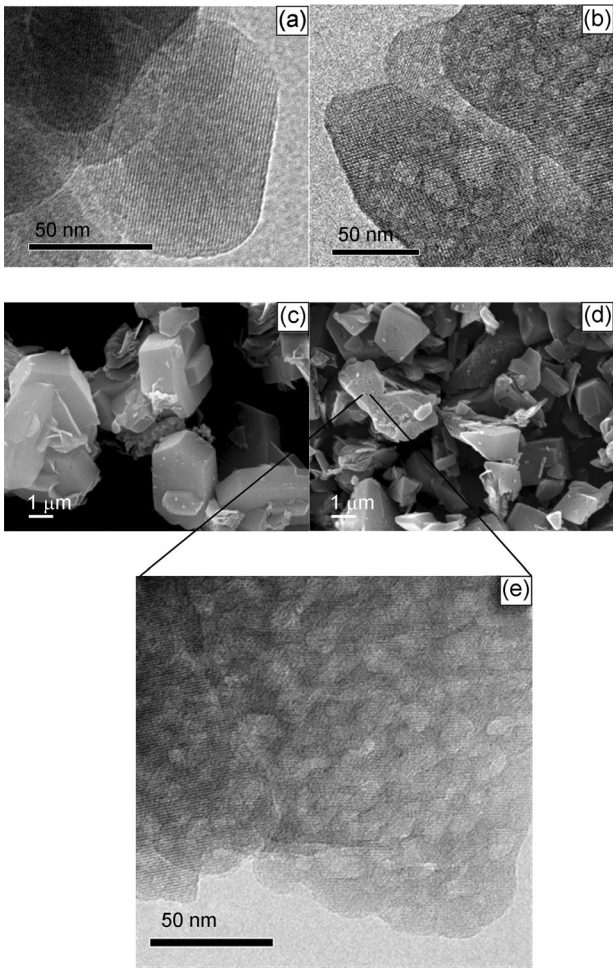

Figure 1. HR-TEM micrographs of a) MOR and b) deAlmm-MOR, SEM micrographs of c) ZSM-5(I) and d) deAlmm-ZSM-5(I), and e) the HR-TEM micrograph of deAlmm-ZSM-5(I).

micropores. The FTIR spectra of adsorbed DTBPy showed the absence of acid sites on the external surface of the zeolite, as the intensity of the band of Brønsted acid sites were

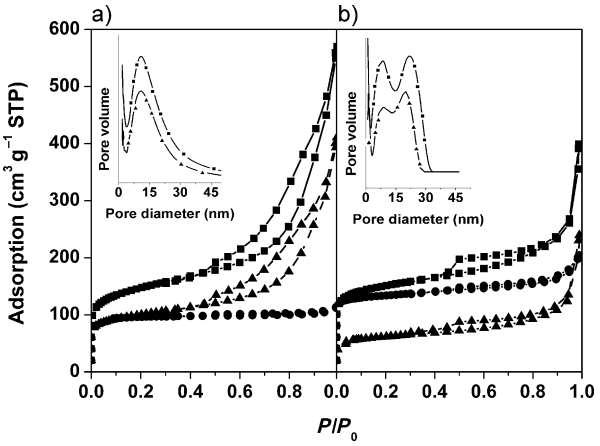

Figure 2. N_2-sorption isotherms of a) ZSM-5(I) and b) mordenite. Parent zeolites (●) and those obtained by alkaline (▲) and subsequent acid leaching (■).

identical before and after DTBPy adsorption. The parallel presence of Brønsted sites detected by [D_3]acetonitrile indicated that the acid sites are located in micropores. The ^{27}Al magic-angle-spinning NMR (MAS-NMR) spectra of deAlmm-ZSM-5(I) also indicated that more than 95% of the Al had tetrahedral coordination in the framework.

The above analysis showed that the creation of mesopores through alkaline treatment (removal of parts of the Si-rich framework) and subsequent leaching of aluminum by oxalic acid resulted in a micro-mesoporous structure with strongly acidic Brønsted sites predominantly located in the shape-selective environment of the micropores.

The potential of these hierarchical zeolites in acid-catalyzed reactions is demonstrated on hydroisomerization of *n*-heptane, cracking of *n*-hexane, and acylation of anisole with acetic anhydride to *p*-methoxyacetophenone (p-MAP). The effects of the micro-mesoporous structure with dealuminated mesopores on the yield of isomers, conversion, and selectivity in the hydroisomerization of *n*-heptane is depicted in Figure 3. While the conversion of *n*-heptane decreased

Table 1: Characteristics of mordenite and ZSM-5 zeolites.

Sample	Structure	Si/ Al[a]	Si/ Al_{FR}[b]	Si/ $Al_{surface}$[c]	c_{Al}[a] mmol g^{-1}	c_B[d] $cm^3 g^{-1}$	c_L[e] $m^2 g^{-1}$	V_{MI} $cm^3 g^{-1}$	S_{EXT} nm	V_{MESO}	D_{MAX}
ZSM-5(I)	microporous	22.2	23.5	14.8	0.72	0.50	0.10	0.15	8	–	–
mm-ZSM-5(I)	micro-meso-porous	8.5	17.4	7.7	1.76	0.31	0.47	0.076	172	0.60	11
deAlmm-ZSM-5(I)	dealuminated micro-meso-porous	81.0	93	105	0.20	0.17	0.02	0.12	250	0.81	11
ZSM-5(II)	microporous	73	80	65	0.23	0.18	0.03	0.16	45	0.06	10
MOR	microporous	12.1	12.5	10.0	1.27	1.10	0.1	0.19	51	0.14	9
mm-MOR	micro-meso-porous	8.7	10.2	7.2	1.71	0.78	0.2	0.06	79	0.31	10
deAlmm-MOR	dealuminated micro-meso-porous	54.9	65	90	0.30	0.15	0.05	0.17	150	0.47	10

[a] From chemical analysis. [b] From ^{29}Si MAS-NMR. [c] From XPS. [d] Concentrations of Brønsted acid sites. [e] Concentration of Lewis acid sites. [d,e] From FTIR spectra of adsorbed [D_3]acetonitrile.

 © 2013 Wiley-VCH Verlag GmbH & Co. KGaA, Weinheim

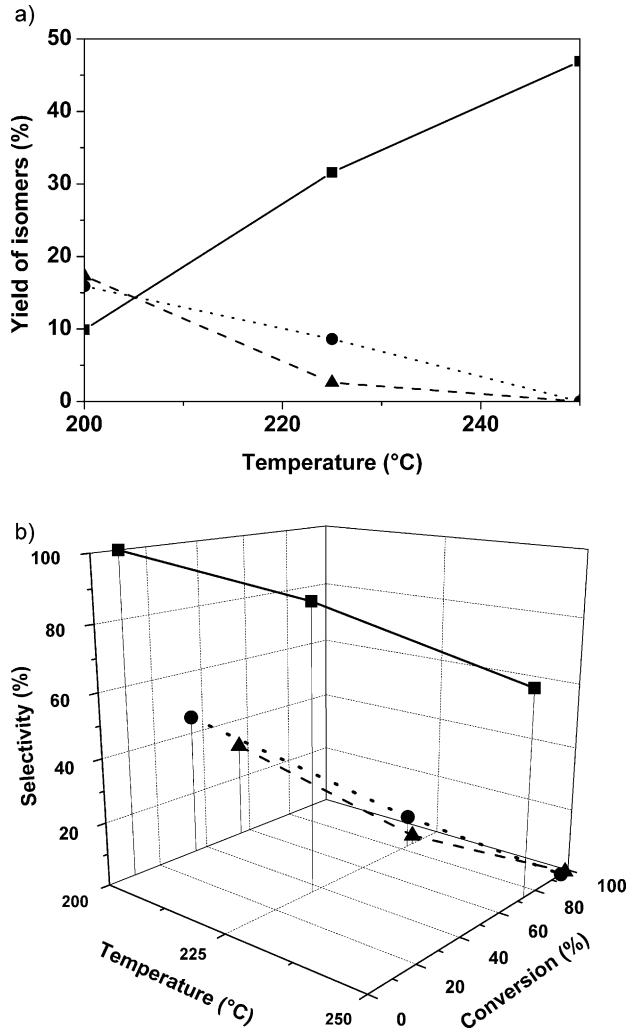

Figure 3. Hydroisomerization of *n*-heptane over PtH-MOR (●), PtH-mm-MOR (▲), and PtH-deAlmm-MOR (■). a) Yields of heptane isomers (sum of mono-, di-, and tribranched isomers), and b) variation of *n*-heptane conversion and selectivity for isoheptane with temperature.

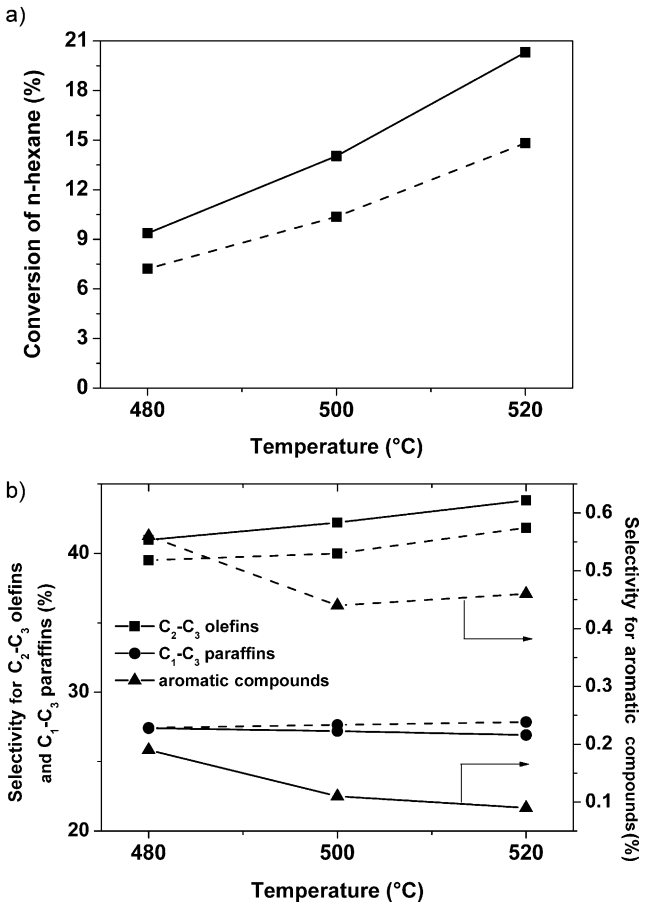

Figure 4. Cracking of *n*-hexane over deAlmm-ZSM-5(I) (solid line) and microporous ZSM-5(II) (dashed line). a) Conversion of *n*-hexane and b) selectivity for C_2-C_3 olefins, C_1-C_3 paraffins, and aromatic compounds as a function of temperature.

slightly (note the considerable decrease in the concentration of the acid sites) for PtH-deAlmm-MOR compared to PtH-MOR, the yield of isoheptanes increased substantially (Figure 3A). This is a result of the dramatic increase in selectivity from PtH-MOR to PtH-deAlmm-MOR (Figure 3B). Figure 4 depicts the effect of dealumination on the conversion and selectivity in cracking of *n*-hexane. As the conversion and product composition of the cracking reaction depend strongly on the concentration of protonic sites, we compared the hierarchical zeolite with the microporous sample that exhibits similar concentration of protonic sites. The dealuminated micro-mesoporous ZSM-5 zeolite provided higher conversion of *n*-hexane and higher selectivity for the desired C_2 and C_3 olefins, and lower selectivity for aromatic compounds. This effect can be explained by the mutual improvement of the mass transport in shorter microporous channels and the shorter contact time of the intermediates inside the channels; thus limiting their further transformation to aromatic compounds, as well as the predominance of protonic sites located in the shape-selective environment of the micropores, suppressing hydrogen-transfer reactions that lead to aromatic compounds. Table 2 shows a double increase in the conversion of anisole acylation by acetic anhydride (from 8 to 15.9%) after ZSM-5 desilication, comparable with Ref. [15] (from about 10 to 20%) under similar conditions. The subsequent acid leaching caused a dramatic increase in conversion to 88% with maintenance of high selectivity (98%) for *p*-methoxyacetophenone. Both the transport through mesopores and reduced concentration of acid sites can contribute to this positive effect in the acylation reaction. The hierarchical shape-selective zeolites with dealuminated mesopores and Brønsted sites in the micropores provided the desired products in high yields in the representative acid-

Table 2: Acylation of anisole with acetic anhydride to *p*-methoxyacetophenone (p-MAP) over ZSM-5.

	Conversion of Ac_2O [%]		Selectivity for *p*-MAP [%]	
Sample	3 h	24 h	3 h	24 h
ZSM-5(I)	8.0	16.4	100	100
mm-ZSM-5(I)	15.9	85.2	96.7	97.1
deAlmm-ZSM-5(I)	88.9	98.2	98.3	98.6

© 2013 Wiley-VCH Verlag GmbH & Co. KGaA, Weinheim

catalyzed reaction as a result of synergism of the enhanced rate of reactant/product transport and presence of acid sites in the shape-selective confined space of the micropores.

Experimental Section

Mordenite (CBV 20A, Lot. No. 20A AD-29–1) and ZSM-5 zeolite (CBV1502 Id. No. 119-90-003) with Si/Al = 12.1 and 73, respectively, were provided by Zeolyst, and ZSM-5 (SM-55) with Si/Al = 22.2 was purchased from AlSi-Penta Zeolithe GmbH. Mordenite and ZSM-5 zeolites with Si/Al = 12.1 and 22.2, respectively, were treated with alkaline solutions (30 mL 0.2 M NaOH per 1 g mordenite stirred in a beaker at 85 °C for 2 h, and 100 mL 0.13 M NaOH per 1 g ZSM-5 at 80 °C for 18 h) and subsequently with acid solution (100 mL 0.5 M oxalic acid per 1 g alkaline-treated zeolite stirred in a beaker at 80 °C for 20 h). All the zeolites were ion-exchanged with 0.5 mol dm^{-3} NH_4NO_3 at RT (1 g of a zeolite per 100 cm^3 of solution, three times over 12 h). Mordenites in the NH_4^+ form were impregnated with an aqueous solution of hexachloroplatinic acid $H_2PtCl_6 \cdot H_2O$ and activated in O_2 at 475 °C for 3 h and in H_2 at 250 °C for 1 h to obtain Pt-H-mordenite (1 wt.% Pt). Zeolites were characterized by XRD (Siemens 5005 diffractometer) (see the Supporting Information, Supplement I), N_2 adsorption at −196 °C (Micromeritics ASAP 2020) (Supplement II), HR-TEM (JEOL JEM 3010), SEM (Jeol JSM-03), ^{27}Al and ^{29}Si MAS-NMR (Bruker Avance 500 MHz spectrometer using 4 mm o.d. ZrO_2 rotors with a rotation speed of 5 kHz, a $\pi/6$ (1.7 μs) excitation pulse, and a relaxation delay of 30 s for ^{29}Si MAS-NMR and 12 kHz and high-power decoupling pulse sequences with $\pi/12$ (0.7 μs) excitation pulses for ^{27}Al MAS-NMR) (Supplements III and IV), FTIR spectroscopy of adsorbed d_3-acetonitrile and 2,6-ditertbutylpyridine (Nexus 670 spectrometer with a resolution of 2 cm^{-1}) (Supplement V) and XPS (ESCA III Mk2 spectrometer). Hydroisomerization of *n*-heptane (WHSV 0.35 h^{-1}, volume H_2/*n*-heptane 80) and cracking of *n*-hexane (WHSV 4 h^{-1}) were performed in a through-flow micro-reactor at atmospheric pressure, and acylation of anisole with acetic anhydride to *p*-methoxyacetophenone in a stirred batch reactor (80 mmol anisole, 10 mmol Ac_2O, 50 mg catalyst, 100 °C). Each catalytic experiment was done 3 times. The reproducibility of kinetic data was estimated (± 5) rel%.

Received: August 14, 2012
Published online: January 9, 2013

Keywords: alkylation · cracking · dealumination · isomerization · zeolites

[1] M. Hartmann, *Angew. Chem.* **2004**, *116*, 6004; *Angew. Chem. Int. Ed.* **2004**, *43*, 5880.
[2] A. Inayat, I. Knoke, E. Spiecker, W. Schwieger, *Angew. Chem.* **2012**, *124*, 1998; *Angew. Chem. Int. Ed.* **2012**, *51*, 1962.
[3] M. Choi, K. Na, J. Kim, Y. Sakamoto, O. Terasaki, R. Ryoo, *Nature* **2009**, *461*, 246.
[4] X. Y. Zhang, D. X. Liu, D. D. Xu, S. Asahina, K. A. Cychosz, K. V. Agrawal, Y. Al Wahedi, A. Bhan, S. Al Hashimi, O. Terasaki, M. Thommes, M. Tsapatsis, *Science* **2012**, *336*, 1684.
[5] W. Fan, M. A. Snyder, S. Kumar, P. S. Lee, W. C. Yoo, A. V. McCormick, R. Lee Penn, A. Stein, M. Tsapatsis, *Nat. Mater.* **2008**, *7*, 984.
[6] C. Madsen, C. J. H. Jacobsen, *Chem. Commun.* **1999**, 673.
[7] D. H. Park, S. S. Kim, H. Wang, T. J. Pinnavaia, M. C. Papapetrou, A. A. Lappas, K. S. Triantafyllidis, *Angew. Chem.* **2009**, *121*, 7781; *Angew. Chem. Int. Ed.* **2009**, *48*, 7645.
[8] K. P. De Jong, J. Zecevic, H. Friedrich, P. E. De Jongh, M. Bulut, S. Van Donk, R. Kenmogne, A. Finiels, V. Hulea, F. Fajula, *Angew. Chem.* **2010**, *122*, 10272; *Angew. Chem. Int. Ed.* **2010**, *49*, 10074.
[9] J. C. Groen, W. Zhu, S. Brouwer, S. J. Huynink, F. Kapteijn, J. A. Moulijn, J. Perez-Ramirez, *J. Am. Chem. Soc.* **2007**, *129*, 355.
[10] J. C. Groen, J. A. Moulijn, J. Perez-Ramirez, *J. Mater. Chem.* **2006**, *16*, 2121.
[11] J. Pérez-Ramírez, *Nat. Chem.* **2012**, *4*, 250.
[12] P. Sazama, B. Wichterlova, J. Dedecek, Z. Tvaruzkova, Z. Musilova, L. Palumbo, S. Sklenak, O. Gonsiorova, *Microporous Mesoporous Mater.* **2011**, *143*, 87.
[13] J. C. Groen, L. A. A. Peffer, J. A. Moulijn, J. Perez-Ramirez, *Chem. Eur. J.* **2005**, *11*, 4983.
[14] R. Caicedo-Realpe, J. Perez-Ramirez, *Microporous Mesoporous Mater.* **2010**, *128*, 91.
[15] D. P. Serrano, R. A. Garcia, G. Vicente, M. Linares, D. Prochazkova, J. Cejka, *J. Catal.* **2011**, *279*, 366.

 © 2013 Wiley-VCH Verlag GmbH & Co. KGaA, Weinheim